CHEMISTRY
A EUROPEAN JOURNAL

DOI: 10.1002/chem.201000015

Coumarin-Caged Rosamine Probes Based on a Unique Intramolecular Carbon–Carbon Spirocyclization

Weiying Lin,* Lingliang Long, Wen Tan, Bingbing Chen, and Lin Yuan[a]

To investigate the biochemistry of life, it is essential to have suitable chemical tools that are able to provide spatiotemporal information because the interactions of biomolecules in living systems are under precise temporal and spatial control. Masking the key functional groups of biomolecules with photolabile protecting groups may afford caged compounds, which are essentially biologically inert.[1] However, upon photolysis, the photolabile groups are deprotected to release the native, active biomolecules. Since light is able to access/activate the desired excitation site at any time, it is then possible to regulate these biomolecules with high temporal and spatial resolution by using the photocaging technology. Caged fluorophore probes are essentially nonfluorescent and can be converted into highly fluorescent species after photolysis.[2] This light-mediated fluorescence-enhancement method, with the intrinsic advantage of high spatiotemporal resolution, renders caged fluorophore probes very useful for studying cell lineage,[3] cell–cell communication,[4] cellular protein fluorescence labeling,[2a] hydrodynamic properties of the cytoplasmic matrix, and lateral diffusion in membranes.[5] Thus, the development of new caged fluorophore probes is very important for studies of molecular and cellular dynamics.

Xanthene fluorophores, such as fluoresceins, rhodamines, and TokyoGreens have been caged. Typically, caged fluorescein (Scheme 1a) or caged rhodamine probes (Scheme 1b) are prepared by incorporating nitrobenzyl groups on the hydroxyl or amino groups of the xanthene core to form deconjugated and nonfluorescent cyclic lactone structures.[2a,6,7] Recently, in an elegant piece of work, Nagano's group reported nitrobenzyl-caged TokyoGreens by exploiting the fluorescence quenching effect of nitro groups.[8] However, the nitrobenzyl-caged xanthenes have several drawbacks. First, the photolytic efficiency (the efficiency of photolysis is defined by the product of the uncaging quantum yield and the extinction coefficient)[9] of these nitrobenzyl-caged xanthenes are very low (typically less than 100).[10] This is highly unfavorable for bio-applications because the intense light that is employed to photolyze caged probes with low photolytic efficiency may be detrimental to living species.[11] Second, the photolabile nitrobenzyl groups have to be removed by UV light, which can cause photodamage to cells, such as changes in morphology and phenotypes, or can even kill cells. Third, the parent dyes of caged fluoresceins suffer from photobleaching.[2a,b] Thereby, these shortcomings have apparently constrained the potential bio-applications of these caged probes.

Rosamines are another key class of xanthenes with favorable photophysical properties. Structurally, in comparison to rhodamines, rosamines lack a carboxylic acid functional group.[12] Thus, the traditional rhodamine caging method is not applicable for rosamines, since they can not lactonize to turn off the fluorescence due to the lack of a carboxylic acid group. To the best of our knowledge, rosamines have not been successfully caged yet. Herein, we introduce the first photocaging strategy for rosamines based on new photocaging chemistry, that is, a unique intramolecular carbon–carbon spirocyclization (Scheme 1c). For proof of concept, rosamine (**3**) was caged with the photolabile coumarin-4-ylmethyl moieties as the representative examples of the novel class of photocaged rosamine probes. Compound **3** is highly fluorescent with red emission at 577 nm. Our hypothesis was that the hydroxyl chemical handle of **3** could allow the incorporation of the photolabile coumarins by alkylation, and the 4-ylmethyl group of the coumarin intermediate could be deprotonated under basic conditions and the resulting nucleophilic carbon (C2′) could attack the electrophilic carbon (C9) of the xanthene core to undergo an intramolecular carbon–carbon spirocyclization. This should render caged probes **1** and **2** nonfluorescent because the conjugation of the xanthene ring is destroyed. Since coumarin-4-ylmethyl derivatives are known to be efficiently photolyzed under

[a] Prof. W. Lin, L. Long, W. Tan, B. Chen, L. Yuan
State Key Laboratory of Chemo/Biosensing and Chemometrics
College of Chemistry and Chemical Engineering, Hunan University
Changsha, Hunan 410082 (P.R. China)
Fax: (+86) 731-8882-1464
E-mail: weiyinglin@hnu.cn

Supporting information for this article is available on the WWW under http://dx.doi.org/10.1002/chem.201000015.

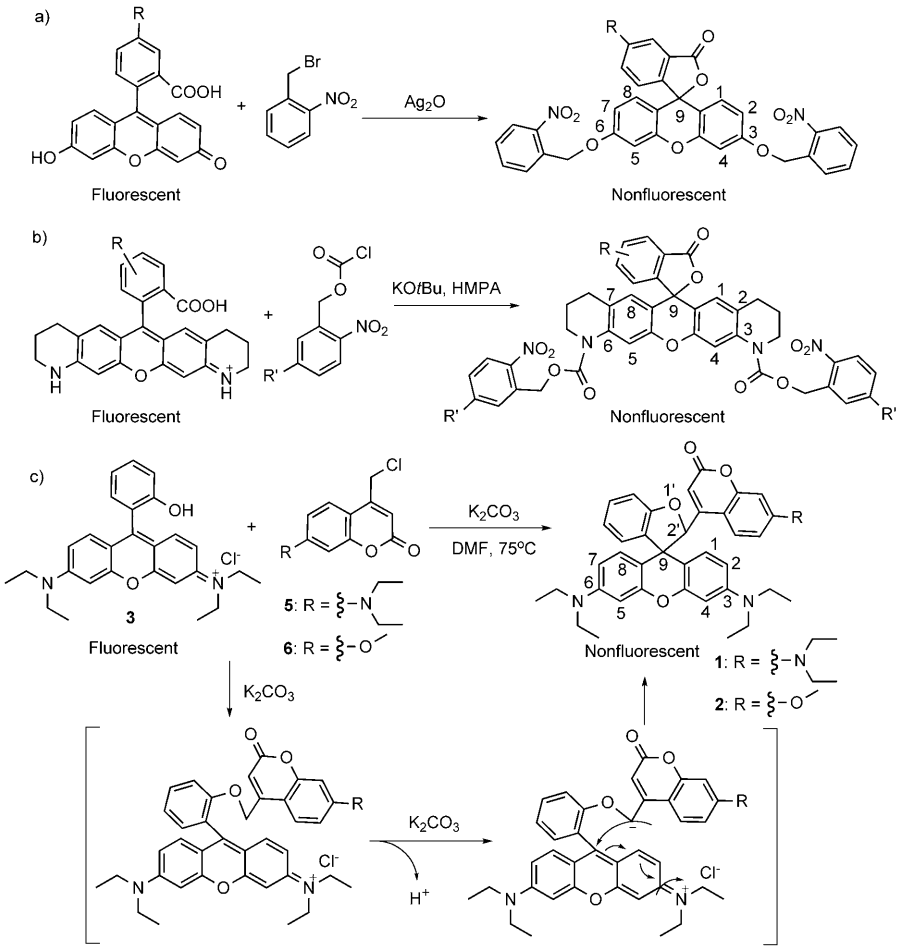

Scheme 1. a) Caging chemistry of fluoresceins; b) Caging chemistry of rhodamines (HMPA = hexamethylphosphoramide); c) New caging chemistry of rosamine: mechanistic design and synthesis of coumarin-caged rosamine probes **1** and **2**.

visible light,[13] we envisioned that the caged probes may be uncaged to release the fluorescent conjugated xanthene ring upon exposure to visible light.

The synthetic routes to the new coumarin-caged rosamine derivatives **1** and **2** are outlined in Scheme 1c and Figure S1 in the Supporting Information. Alkylation of **3** with coumarins **5** or **6** provided coumarin-caged rosamines **1** or **2**, respectively, in 48 or 55% yield. Reference coumarin aldehydes **7** and **8** (Figure S1 in the Supporting Information) were also prepared by the standard chemistry.

The structures of the novel coumarin-caged rosamine probes **1** and **2** were fully characterized by ^{1}H and ^{13}C NMR spectroscopy (Figures S2–S5 in the Supporting Information), and HRMS. Furthermore, the X-ray crystallographic analysis authenticated that, indeed there is a carbon–carbon spirocyclic structure in both the caged probes **1** and **2** (Figure S6 in the Supporting Information). Thus, the novel carbon–carbon spirocyclic structure in the caged probes **1** and **2** indicates that they represent a new class of xanthene-based spirocyclic derivatives. Notably, the formation of the carbon–carbon spirocyclic ring clearly confines the xanthene ring to the deconjugated form. Although the fluorescence of xanthenes can be switched off by xanthene deconjugation through the formation of the deconjugated cyclic lactone or lactam structure[2a,6,7,14] or the zinc coordinated μ-oxygen structure,[15] these methods are apparently not applicable for photocaging rosamines.

In the absence of light, caged probe **1** displayed only the characteristic absorption of 7-*N*,*N*-diethylaminocoumarin around 400 nm with a molar extinction coefficient of $21\,300\,M^{-1}cm^{-1}$ under the neutral aqueous conditions (25 mM sodium phosphate buffer, pH 7.0, containing 10% DMF as a cosolvent) (Figure S7 in the Supporting Information). However, the typical absorption of conjugated rosamine dyes around 550 nm was not observed. This is in good agreement with the carbon–carbon spirocyclic structure, which obviously breaks the conjugation of the xanthene moiety in the caged species. A similar absorption profile was also noticed for caged probe **2** (Figure S8 in the Supporting Information). However, caged probe **2** has much lower absorption in the visible region than caged probe **1**. Consequently, we decided to focus on caged probe **1** for further spectroscopic and photolysis studies. Upon visible light photolysis (the inexpensive and simple-to-use 275 W tungsten lamp with a visible light bandpass filter (390–600 nm) was chosen as the visible light source[16]), the typical conjugated xanthene absorption at around 554 nm increased gradually in a light-exposure and time-dependent manner indicating the formation of a conjugated rosamine species.

Probe **1** showed no emission in the rosamine emission region, consistent with the formation of the deconjugated carbon–carbon spirocyclic structure. In contrast, upon exposure to visible light, a dramatic fluorescence enhancement at 577 nm was observed (Figure 1), indicating the formation of a conjugated rosamine species. Notably, visible light exposure on caged probe **1** induced a large fluorescence enhancement (360-fold), which is much larger than that of a nitrobenzyl caged rhodamine (<50-fold).[7b] Such a magnitude of fluorescence jump after a brief photolysis is desirable for cellular fluorescence imaging applications.[8] In addition, the uncaging also resulted in light-exposure and time-

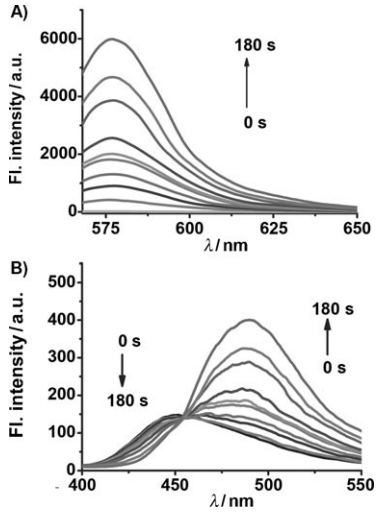

Figure 1. The emission spectra of probe **1** (0.6 μM in 25 mM sodium phosphate buffer, pH 7.0, containing 10% DMF) prior to exposure to visible light, and after increasing duration of illumination with visible light. A) Emission changes in the rosamine emission region with $\lambda_{ex}=554$ nm (ex = excitation); B) Emission changes in the coumarin emission region with $\lambda_{ex}=396$ nm. The duration of light exposure is in seconds.

dependent changes in the coumarin emission spectra: a large fluorescence increase accompanied by a redshift from 450 to 490 nm. Interestingly, an isoemission point at 454 nm was noted implying that only one new coumarin species was formed upon visible light illumination.

To investigate the identity of the photolysis products, the solutions of probe **1** before and after different durations of visible light exposure were subjected to HPLC analysis (Figure S9 in the Supporting Information), which indicates that caged probe **1** generated rosamine **3** and coumarin **7** after visible light exposure. The character of the photolysis products was further substantiated by mass spectrometric analysis. The expected molecular peaks at 415.2 $[\mathbf{3}]^+$ and 278.0 $[\mathbf{7}+CH_3OH+H]^+$ were displayed in the mass spectrum of a partially photolyzed solution of probe **1** (Figure S10 in the Supporting Information). Furthermore, the emission and excitation spectra of probe **1** after exhaustive photolysis are identical to those of standard **3** and **7** when excited or monitored at the appropriate wavelengths (Figures S11 and S12 in the Supporting Information). Thus, the HPLC, mass spectrometry, and emission and excitation spectroscopy studies confirmed that the uncaging of caged probe **1** afforded **3** and **7** (Figure S13 in the Supporting Information). Interestingly, upon exposure of caged probe **1** to visible light in the presence of hydroquinone (a free-radical scavenger), almost no fluorescence enhancement in both the rosamine and coumarin channels was observed (Figure S14 in the Supporting Information). The preliminary finding that a free-radical scavenger could completely inhibit the photolysis of caged **1** suggests that a radical mechanism is likely to be involved in the photolysis. Based on this preliminary study and the photochemistry of coumarin-4-ylmethyl derivatives[1a,17] and dihydrorosamine,[18] a probable mechanism of photorelease was proposed (Figure S15 in the Supporting Information).

The uncaging quantum yield of probe **1** was calculated to be 0.26 by means of HPLC analysis (see the Supporting Information), and was comparable to other 4-methyl-7-*N*,*N*-diethylaminocoumarin caged species.[13b] The photolytic efficiency of caged probe **1** is 5538. In contrast, the photolytic efficiencies of nitrobenzyl-caged fluoresceins are only around 60.[10] Thus, the photolytic efficiency of caged probe **1** is about a hundred times larger than those of caged fluoresceins. We concluded that caged probe **1** is superior to caged fluoresceins in terms of photolytic efficiency.

The fluorescence quantum yields of **3** and **7** were determined as 0.20 and 0.10, respectively (see the Supporting Information). In addition, we also evaluated the photostability of the photolyzed product **3**, under visible light illumination. The fluorescence spectra of **3** are practically the same after 15 min of illumination under the tungsten lamp (Figure S16 in the Supporting Information), suggesting that the photolyzed product is highly resistant to photobleaching. This is in contrast with the parent dyes of caged fluoresceins, which are prone to photobleaching.[2a–b]

Since the utility of caged dyes depends on their hydrolytic stability at physiological pH in the absence of light, we examined the rosamine emission of caged probe **1** in phosphate-buffered saline (PBS) in the dark. After three weeks, essentially no rosamine fluorescence emission was observed (Figure S17 in the Supporting Information), indicating that probe **1** was very stable in the absence of light. Thus, caged probe **1** has a low fluorescence background in the rosamine emission region due to the high stability of the carbon–carbon spirocyclic structure at physiological pH in the dark.

To examine the photoactivation of caged probe **1** in cell-based systems, Hela cells were incubated with caged probe **1** (1 μM) and the selected cells were photolyzed by visible light through a fluorescence microscope.[2a,8] After photolysis for 10 s, the illuminated cells showed intense red emission (Figure 2B, for a color version, see Figure S19 in the Supporting Information) and green emission (Figure 2C) in the rosamine and coumarin emission regions, respectively. In contrast, no fluorescence was observed in the cells that were not photolyzed. These data established that probe **1** is cell-membrane permeable and can be employed for spatial control imaging in living cells.[19] The cells exhibited no apparent cytotoxicity after photo-uncaging. For comparison, when the cells were incubated with **3** (the parent dye of caged probe **1**), all the cells exhibited bright red fluorescence (Figure 2J), indicating no spatial-restricted imaging, since the fluorescence of **3** is not amenable to light regulation. Thus, probe **1** displayed an advantage over **3** in that the imaging of probe **1** is light controllable.

In conclusion, we have reported the first photocaging strategy for rosamines based on novel photocaging chemistry, that is, an intramolecular carbon–carbon spirocyclization. The formation of the carbon–carbon spirocyclic structure in the caged probes **1** and **2** has been unambiguously characterized by ^1H and ^{13}C NMR spectroscopy, HRMS, X-

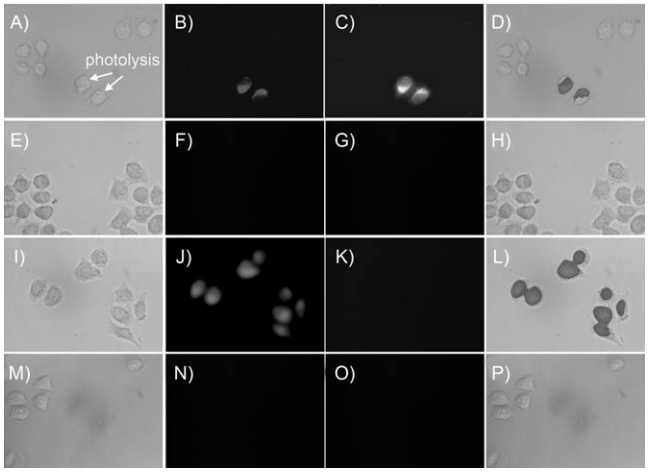

Figure 2. Local uncaging and imaging of probe **1** in living cells. A) Brightfield image of Hela cells incubated with probe **1**. B) and C) Fluorescence images of the cells in panel A) in the rosamine (λ_{ex} = 562 nm, λ_{em} = 604 nm; em = emission) and coumarin (λ_{ex} = 416 nm, λ_{em} = 535 nm) emission channels, respectively, after 10 s illumination of the selected cells. D) Overlay of images A) and B). E) Brightfield image of Hela cells incubated with probe **1** without illumination. F) and G) Fluorescence images of the cells in panel E) in the rosamine and coumarin emission channels, respectively. H) Overlay of images E) and F). I) Brightfield image of Hela cells incubated with rosamine **3**. J) and K) Fluorescence images of the cells in panel I in the rosamine and coumarin emission channels, respectively. L) Overlay of images I) and J). M) Brightfield image of Hela cells only (in the absence of probe **1**). N) and O) Fluorescence images of the cells in panel M in the rosamine and coumarin emission channels, respectively. P) Overlay of images M) and N).

ray crystallographic analysis, and absorption and emission spectra. We also demonstrated that upon local photoactivation by visible light, caged probe **1** could release **3** and **7** for living cell fluorescence imaging in a light-dependent fashion. In comparison with the nitrobenzyl caged xanthenes, our newly constructed carbon–carbon spirocyclic probes clearly exhibited several significant advantages: high photolytic efficiency, photoactivation by visible light instead of UV light, and high photostability of the parent dyes. Thus, these highly favorable photochemical properties should render the novel caged probes powerful chemical tools for studies of the spatiotemporal dynamics of a wide variety of biological processes. In addition, the general and novel rosamine photocaging strategy could be widely applicable for caging other classes of the xanthene family that also lack a carboxylic acid group with the various photolabile groups susceptible to diverse uncaging conditions.

Acknowledgements

Funding was partially provided by NSFC (20872032 and 20972044), NCET (08-0175), and the Key Project of the Chinese Ministry of Education (no.: 108167).

Keywords: cage compounds · dyes/pigments · fluorescent probes · photoactivation · photolysis

[1] a) *Dynamic Studies in Biology: Phototriggers, Photoswitches and Caged Biomolecules* (Eds.: M. Goeldner, R. Givens), Wiley-VCH, Weinheim, **2005**; b) H. Lee, D. R. Larson, D. S. Lawrence, *ACS Chem. Biol.* **2009**, *4*, 409–427.

[2] a) T. J. Mitchison, K. E. Sawin, J. A. Theriot, K. Gee, A. Mallavarapu, in *Methods in Enzymology, Vol. 291* (Eds.: G. Marriot), Academic Press, New York, pp. 63–78; b) Y. Zhao, Q. Zheng, K. Dakin, K. Xu, M. L. Martinez, W. Li, *J. Am. Chem. Soc.* **2004**, *126*, 4653–4663; c) G. Zheng, Y. Guo, W. Li, *J. Am. Chem. Soc.* **2007**, *129*, 10616–10617.

[3] a) D. J. Kozlowski, T. Murakami, R. K. Ho, E. S. Weinberg, *Biochem. Cell Biol.* **1997**, *75*, 551–562; b) J. Vincent, P. H. O'Farrell, *Cell* **1992**, *68*, 923–931.

[4] a) Y. Guo, S. Chen, P. Shetty, G. Zheng, R. Lin, W. Li, *Nat. Methods* **2008**, *5*, 835–841; b) S. Yang, W. Li, *Nat. Protoc.* **2009**, *4*, 94–101; c) K. Dakin, Y. Zhao, W. Li, *Nat. Methods* **2005**, *2*, 55–62; d) K. Svoboda, D. W. Tank, W. Denk, *Science* **1996**, *272*, 716–719.

[5] R. P. Haugland, *Handbook of Fluorescent Probes and Research Chemicals*, 6th ed., Molecular Probes, Eugene, **1996**.

[6] T. J. Mitchison, *J. Cell Biol.* **1989**, *109*, 637–652.

[7] a) K. R. Gee, E. S. Weinberg, D. J. Kozlowski, *Bioorg. Med. Chem. Lett.* **2001**, *11*, 2181–2183; b) J. Ottl, D. Gabriel, G. Marriott, *Bioconjugate Chem.* **1998**, *9*, 143–151.

[8] T. Kobayashi, Y. Urano, M. Kamiya, T. Ueno, H. Kojima, T. Nagano, *J. Am. Chem. Soc.* **2007**, *129*, 6696–6697.

[9] G. C. R. Ellis-Davies, *Nat. Methods* **2007**, *4*, 619–628.

[10] G. A. Krafft, W. R. Sutton, R. T. Cummings, *J. Am. Chem. Soc.* **1988**, *110*, 301–303.

[11] A. Momotake, N. Lindegger, E. Niggli, R. J. Barsotti, G. C. R. Ellis-Davies, *Nat. Methods* **2006**, *3*, 35–40.

[12] L. Wu, K. Burgess, *J. Org. Chem.* **2008**, *73*, 8711–8718.

[13] a) T. Furuta, H. Torigai, M. Sugimoto, M. Iwamura, *J. Org. Chem.* **1995**, *60*, 3953–3956; b) V. Hagen, J. Bendig, S. Frings, T. Eckardt, S. Helm, D. Reuter, U. B. Kaupp, *Angew. Chem.* **2001**, *113*, 1077–1080; *Angew. Chem. Int. Ed.* **2001**, *40*, 1045–1048; c) V. R. Shembekar, Y. Chen, B. K. Carpenter, G. P. Hess, *Biochemistry* **2005**, *44*, 7107–7114.

[14] H. N. Kim, M. H. Lee, H. J. Kim, J. S. Kim, J. Yoon, *Chem. Soc. Rev.* **2008**, *37*, 1465–1472.

[15] A. Ojida, I. Takashima, T. Kohira, H. Nonaka, I. Hamachi, *J. Am. Chem. Soc.* **2008**, *130*, 12095–12101.

[16] W. Lin, H. Frei, *J. Am. Chem. Soc.* **2002**, *124*, 9292–9298.

[17] W. Lin, D. S. Lawrence, *J. Org. Chem.* **2002**, *67*, 2723–2726.

[18] J. E. Whitaker, P. L. Moore, R. P. Haugland, R. P. Haugland, *Biochem. Biophys. Res. Commun.* **1991**, *175*, 387–393.

[19] For global uncaging and imaging of probe **1**, see Figure S18 in the Supporting Information.

Received: January 5, 2010
Published online: March 10, 2010

